NIST Technical Note 1464

Development of a Fast-Response Fire Suppressant Concentration Meter

Erik L. Johnsson
George W. Mulholland
Gerald T. Fraser
Igor I. Leonov
German Y. Golubiatnikov

NIST

National Institute of Standards and Technology
Technology Administration, U.S. Department of Commerce

NIST TN XXXX

Development of a Fast-Response Fire Suppressant Concentration Meter

Erik L. Johnsson
George W. Mulholland
Fire Metrology Group
Fire Research Division
Building and Fire Research Laboratory

Gerald T. Fraser
Optical Thermometry and Spectral Methods Group
Optical Technology Division
Physics Laboratory

Igor I. Leonov
German Y. Golubiatnikov
Institute of Applied Physics,
Russian Academy of Sciences,
Nizhniy Novgorod, Russia

August 2004

CONTENTS

ACKNOWLEDGEMENTS

DISCLAIMER

Certain commercial equipment or instruments are identified in this paper to adequately specify the experimental procedure. This in no way implies endorsement or recommendation by NIST.

ABSTRACT

The measurement of the temporal and spatial distribution of a suppression agent is essential for characterizing the fire extinguishment process and for certifying a fire-suppression system. A time response of 10 ms to 50 ms is required for dry-bay suppression studies and 100 ms to 200 ms for ground-vehicle crew compartment deflagration protection. The Differential Infrared Rapid Agent Concentration Sensor (DIRRACS) is being developed to provide such measurements. The first version of the instrument consisted of an infrared (IR) source, narrow-band pass filter, chopper, and pyroelectric sensor. While the device was capable of providing qualitative data as fast as 30 ms, the device was affected by air flow and had low signal-to-noise ratio and a too-slow time response.

The modified version, DIRRACS II, has been fabricated to overcome these shortcomings by removing the IR source from the flow region, adding a periscope assembly for directing the IR beam into the sample space, and using a faster-response detector. The new design eliminates the previous design's flow sensitivity, increases the signal-to-noise ratio by over 30-fold, and improves time response to less than 10 ms. The data acquisition and analysis system has also been improved. A compact, hardened version of DIRRACS II has been developed as well. DIRRACS II calibration and release test results using HFC-125 as the fire suppressant are presented.

1.0   INTRODUCTION

1.1   MOTIVATION

There is a need for monitoring the concentration of potential halon replacement chemicals with millisecond response time.[1] One scenario of great concern to the Department of Defense is the penetration of an enemy shell into the fuel tank or dry bay of an aircraft. To prevent structural damage to the aircraft wing or fuselage to the point where the plane would be lost, the fire must be extinguished rapidly. This requires that the fire extinguishing agent be distributed throughout the interior region surrounding the fuel tank, the dry-bay, in less than 30 ms. Another application requiring measurement of fire suppressant dispersal is crew compartments in ground vehicles. This application requires that a fire be detected and extinguished fast enough, in about 200 ms, to minimize injury to the occupants.

The instruments currently used for monitoring the concentration of halon 1301 are the Statham analyzer [2] and the Halonyzer [3]. Each is extractive and has a time response on the order of 200 ms or longer and thus they are not capable of monitoring the distribution of the agent in a dry bay type environment at the required temporal resolution. There is a need for an instrument with a much faster time response for monitoring the potential halon replacement chemicals. The design goal is an instrument with a response time of 10 ms or less that could be used with a variety of fire suppression agents over a volume fraction range from 0.01 to 0.20 with an expanded uncertainty of 10 % of the nominal value.

2.0   ORIGINAL INSTRUMENT DESIGN, DIRRACS I

2.1   OVERVIEW

The Differential Infrared Rapid Agent Concentration Sensor (DIRRACS) is a non-dispersive IR absorption instrument which takes advantage of the strong IR absorption near 8 μm to 9 μm by molecules containing C-F bonds. A detailed description of the instrument design and theory of operation is given by Pitts *et al.* [1]. It was first developed at NIST in 1995 as part of a research project to identify optimal commercial replacement for halon 1301 as an extinguishing agent and to develop the necessary diagnostics for testing the candidate replacements. A similar instrument to the DIRRACS was developed by Takeuchi *et al.* [4] for measuring CO_2 and used IR radiation and a modulated signal. The original and latest versions of the DIRRACS will be referred to as DIRRACS I and II, respectively.

2.2   DESCRIPTION

An overall schematic of the original DIRRACS I is shown in Fig. 1. Figure 2 shows a schematic of the optical design. In DIRRACS I, IR radiation from a coil heater source heated to 770 K is emitted in all directions striking a ZnSe window with about 20 % reflection loss. The radiation that passes through the window is directed through a 2.8 cm long sample volume. Some fraction of the IR radiation is absorbed by the agent depending on the concentration. The remaining radiation passes through the ZnS window with some reflection loss before passing through the transmission tube. Then the beam passes through a long-wavelength cut-off filter to remove IR

radiation with a wavelength, λ, longer than 14 μm, through a chopper with a limiting slot size operating at 500 Hz, through a narrow-band pass filter transmitting from 8.4 μm to 8.9 μm, into a conical collector, and onto a LiTaO₃ pyroelectric detector. Each one of these optical components has losses that reduce the IR radiation reaching the detector.
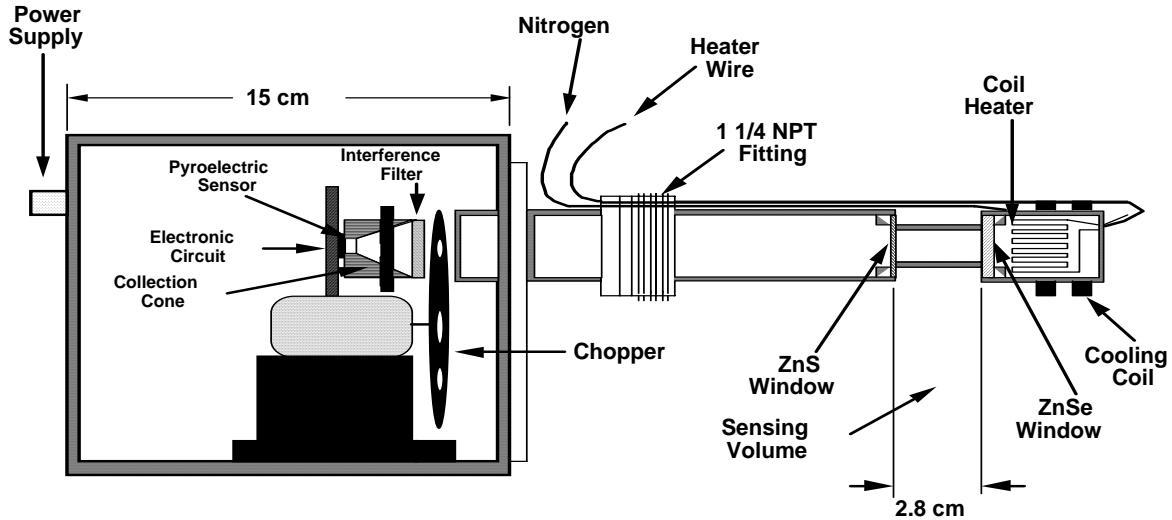
Figure 1. A schematic of the overall design of DIRRACS I
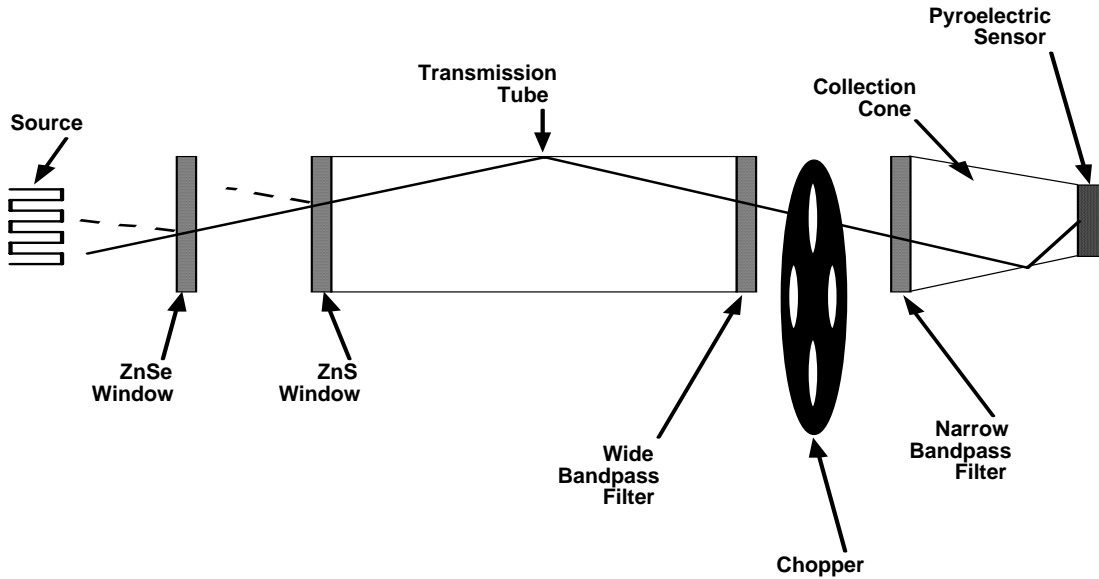
Figure 2. A schematic of the optical design used in DIRRACS I.

The pyroelectric detector has a built-in FET (field-effect transistor) amplifier. The output signal was increased with a 100x low-noise amplifier and frequencies below about 300 Hz were eliminated by a high-pass filter. The detector output was collected at 20 kHz using a digitizing card mounted in a personal computer (PC) and analyzed to determine the peak-to-valley (Pk-Vy) voltage difference. A computer controlled calibration system (described in section 4.1) using three mass flow controllers allowed for calibrating the Pk-Vy signal against HFC-125

2

concentration. For the 2.8 cm optical path length, the instrument responds over a volume fraction range from 0.01 to 0.25.

2.3 THEORY OF OPERATION

As the agent enters the sensing volume, the IR radiation is absorbed by the agent, reducing the flux of radiation reaching the detector. The higher the concentration, the lower the flux that reaches the detector. The IR absorption spectrum of HFC-125/C_2HF_5 is plotted in Fig. 3 for a concentration of 6.3×10^{-3} mol/m^3 with a 10 m path length at a partial pressure of about 16 Pa. Also plotted is the transmission spectrum of the narrow-band pass filter. The spectra plotted in Fig. 3 illustrate that HFC-125 has strong IR absorption features over the 8.4 µm to 8.9 µm transmitted wavelength region of the narrow-band pass filter. This region has little interfering absorption from air constituents. There is also strong IR absorption in the same spectral region for other agents with similar C-F bonds including HFC-227ea/C_3HF_7, FC-218/C_3F_8, halon 1301/CF_3Br, and CF_3I. Halon 1301's strong absorption peak at 9.2 µm corresponds to a fundamental symmetric stretch of the CF_3 (symmetry type A_1, assignment ν_1) [5]. HFC-125 and halon 1301 are the two agents used in this study.
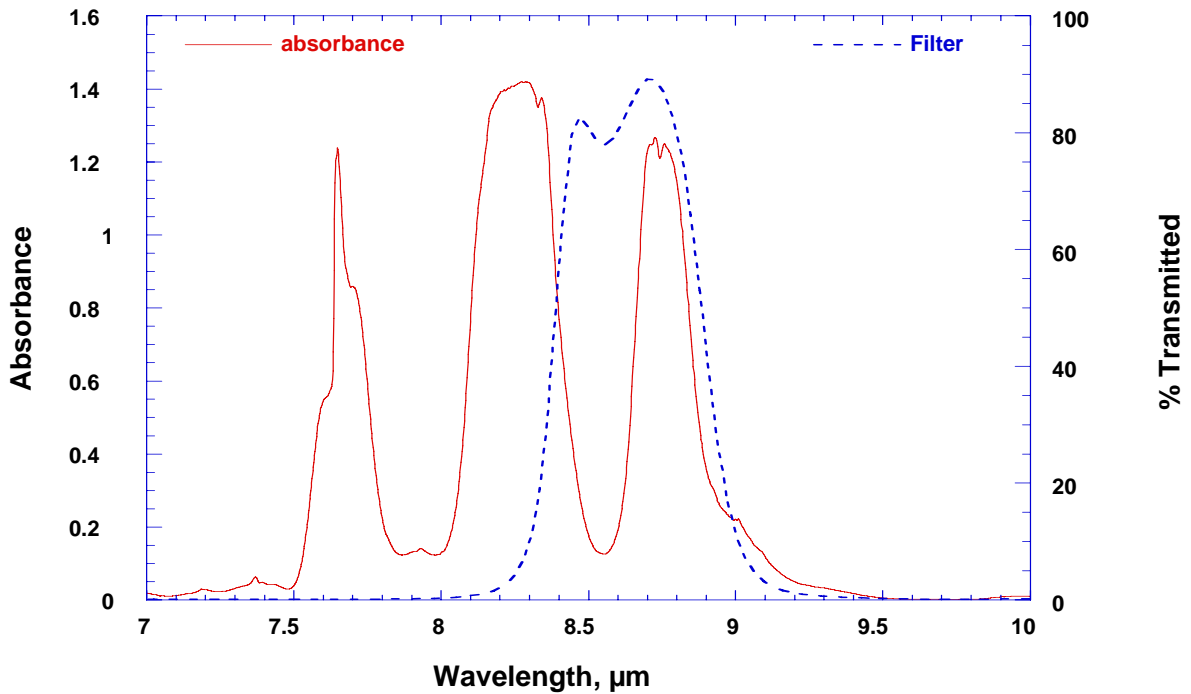
Figure 3. The absorption spectrum of HFC-125 superimposed with the transmittance spectrum for the band pass filter.

The starting point for modeling the IR transmission through the agent is Bouger's law, which relates I_λ^0, the original intensity of incident monochromatic light of wavelength λ, and the intensity of the radiation I_λ transmitted through a path length L of the agent,

$$I_\lambda / I_\lambda^0 = e^{-K(\lambda)CL} \ ,$$ (1)

3

where C is the molar concentration of the agent. The quantity $K(\lambda)$ is the spectral absorption coefficient of the agent. The absorbance, $A(\lambda)$, is related to the transmittance, I_λ/I_λ^0 by:

$$A(\lambda) = -\log_{10}(I_\lambda / I_\lambda^0) \ . \tag{2}$$

From Eqs. (1) and (2), we obtain the following relation between $K(\lambda)$ and $A(\lambda)$:

$$K(\lambda) \approx \frac{2.3 \, A(\lambda)}{C \, L} \ . \tag{3}$$

We make use of this relation in deriving $K(\lambda)$ from the absorbance measurements made for HFC-125.

The coil heater IR source is approximated as a black body radiation source. The black body spectral radiance, L_λ, which has the units of W/(sr m^3), is given by the following equation from Dereniak and Crowe [6]:

$$L_\lambda = \frac{2 \, hc^2}{\lambda^5 \, [\, \exp(hc/\lambda kT) - 1]} \ . \tag{4}$$

In this expression h is Planck's constant (6.62607×10^{-34} J s), c is the speed of light (2.99792×10^8 m/s), k is Boltzmann's constant (1.38065×10^{-23} J/K), and λ is the wavelength of light (m). In Fig. 4 the spectral distributions are plotted for three temperatures including the estimated source temperature, 800 K, and the IR source housing temperature, 330 K. We see that, as expected, the highest temperature source has a greater radiance at all λ.

The goal is to estimate the effect of the concentration of the agent on the radiant heat flux reaching the IR transmission tube. If the source diameter and the transmission-tube diameter are both small relative to the separation distance, the radiant flux incident on the window of the transmission tube is given by:

$$\Phi = L_\lambda \, A_s \, \Omega_d \ , \tag{5}$$

where A_s is the cross section area of the source and Ω_d is the solid angle of the source subtended by the transmission tube. The radiant black body intensity without agent present I_λ^0, defined as the flux per solid angle, is given by:

$$I_\lambda^0 = L_\lambda \, A_s \ . \tag{6}$$

In our case, the diameters of both the source and the transmission tube are comparable to the path length so that Eqs. (5) and (6) are not exact. A full treatment of this optical arrangement would involve integrating over both the source area and the cross section of the transmission tube. However, Eq. (6) is a useful approximation for studying the effects of wavelength and temperature on the radiant intensity reaching the detector. Besides the source, the optical components most sensitive to the wavelength are the narrow and wide band pass filter. We use the quantity $F(\lambda)$ to represent the combined wavelength dependent filter function for both filters. The windows, transmission tube, conical collector, and chopper affect the amount of radiation passing through the device, but are not very sensitive to wavelength.
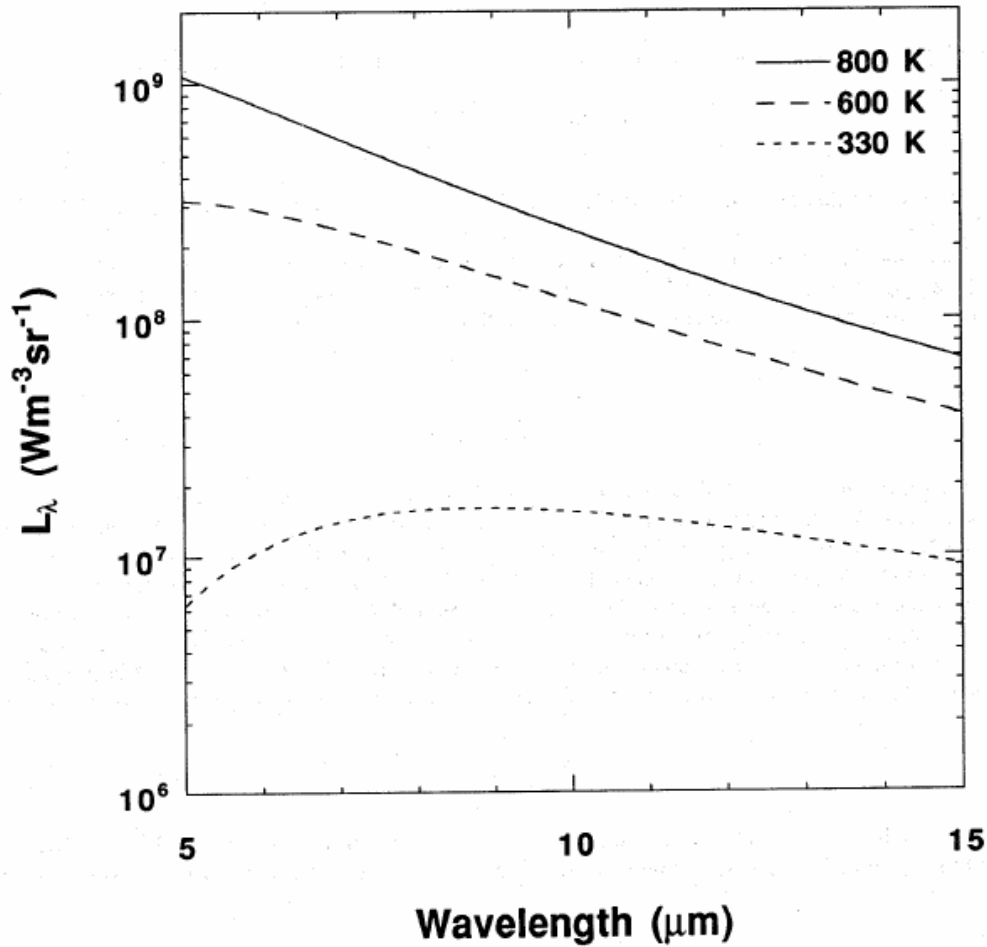
Figure 4. Effect of temperature on black body spectral radiance, L_λ.

Now it is possible to compute the total radiant intensity I_t reaching the transmission tube as a function of agent concentration. This involves integrating the expression for the transmitted intensity over wavelength. The following expression is obtained for the ratio of the total transmitted radiant intensity I_t with agent present to the intensity I_t^0 in the absence of agent:

$$\frac{I_t}{I_t^0} = \frac{\int_{\lambda_1}^{\lambda_2} e^{-K(\lambda)CL}\, I_\lambda^0\, F(\lambda)\, d\lambda}{\int_{\lambda_1}^{\lambda_2} I_\lambda^0\, F(\lambda)\, d\lambda} \tag{7}$$

A FORTRAN program was developed to compute I_t/I_t^0 based on Eq. (7). The program returns the theoretical output of the device for a given concentration of agent. The program first reads in the filename for the spectral absorbance of the agent, the agent concentration, the temperature, and the path length. Next, the program reads the filter transmittance and the absorbance as a function of wavelength. The wavelength corresponding to each absorbance is then converted from wave number in inverse centimeters (as provided) to meters.

An integration loop with a step size of 0.01 μm is started wherein three terms are calculated and combined to generate the light intensities transmitted through the agent and through air as required by Eq. (7). The terms are the exponential term, $e^{-K(\lambda)CL}$, a function of the agent concentration, the intensity term, I_λ^0, a function of wavelength according to Eqs. (4) and (6), and the filter transmittance term, $F(\lambda)$, also a function of wavelength. Integration uses the trapezoidal rule. The light intensity through the agent, I_t, is calculated by summing the product of the exponential, intensity, and filter terms and the wavelength increment. The light intensity through air, I_t^0, is calculated by summing the product of the intensity and filter terms and the wavelength delta. Upon completion of the integration loop, the two intensity sums are divided to generate the fraction of light transmitted through the agent mixture relative to that which would have passed through air. The ratio and intensity sums are written to the screen.

The integration was performed numerically with a step size of 0.01 μm over the wavelength range from 5 μm to 10 μm for a path length of 2.8 cm. The intensity ratio is plotted in Fig. 5 as a function of HFC-125 concentration for three source temperatures. It is seen that the source temperature has very little effect on the intensity ratio.
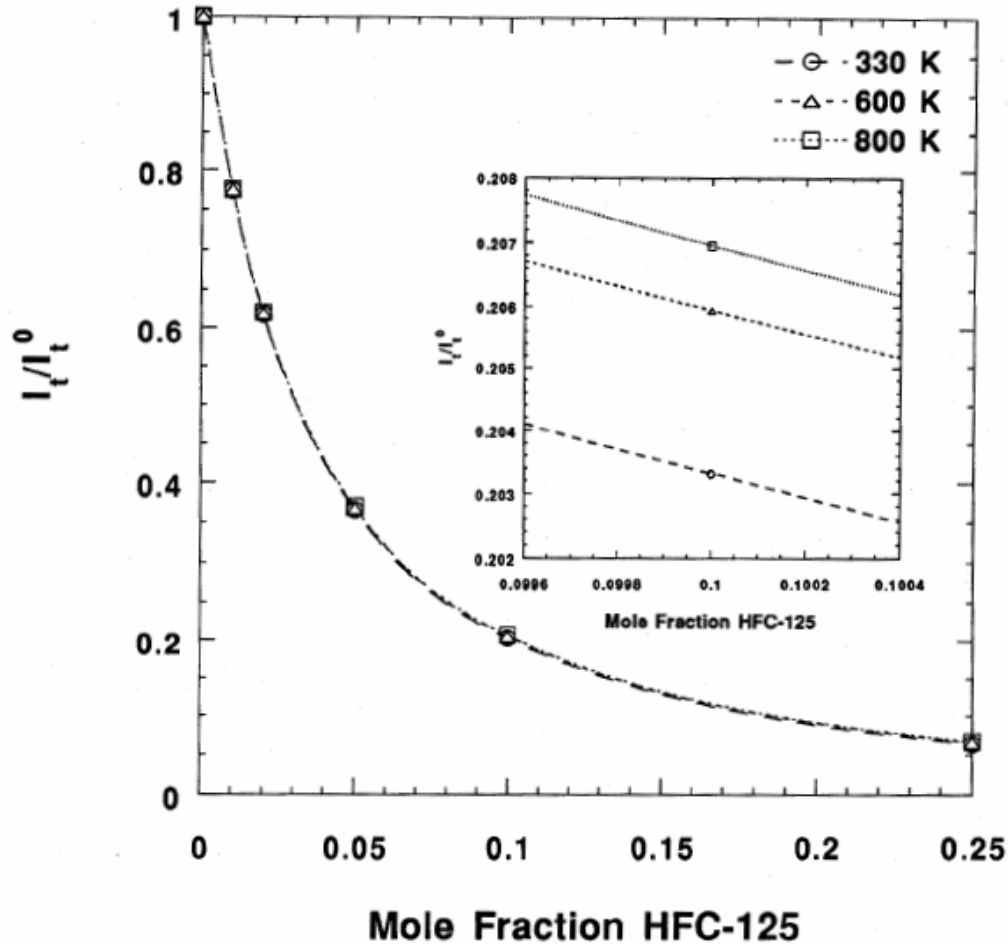
Figure 5. Predicted ratio of the wavelength integrated intensity of the transmitted IR radiation and the incident IR radiation versus volume fraction of HFC-125 for three IR source temperatures. The insert is a magnification of the curves at a volume fraction of 0.1.

6

In Fig. 6, the intensity ratio is plotted for a hypothetical narrow-band pass filter that only allows passage of the radiation at the peak in the absorbance at λ equal to 8.75 μm (see Fig. 3). In this case of a single wavelength, Eq. (7) reduces to Eq. (1) (Bouger's Law). The exponential decrease in the intensity ratio with respect to concentration limits the concentration range that could be measured. Tuning off of the center of the absorption feature increases the concentration range and provides the capability to use the same instrument for measuring several agents.
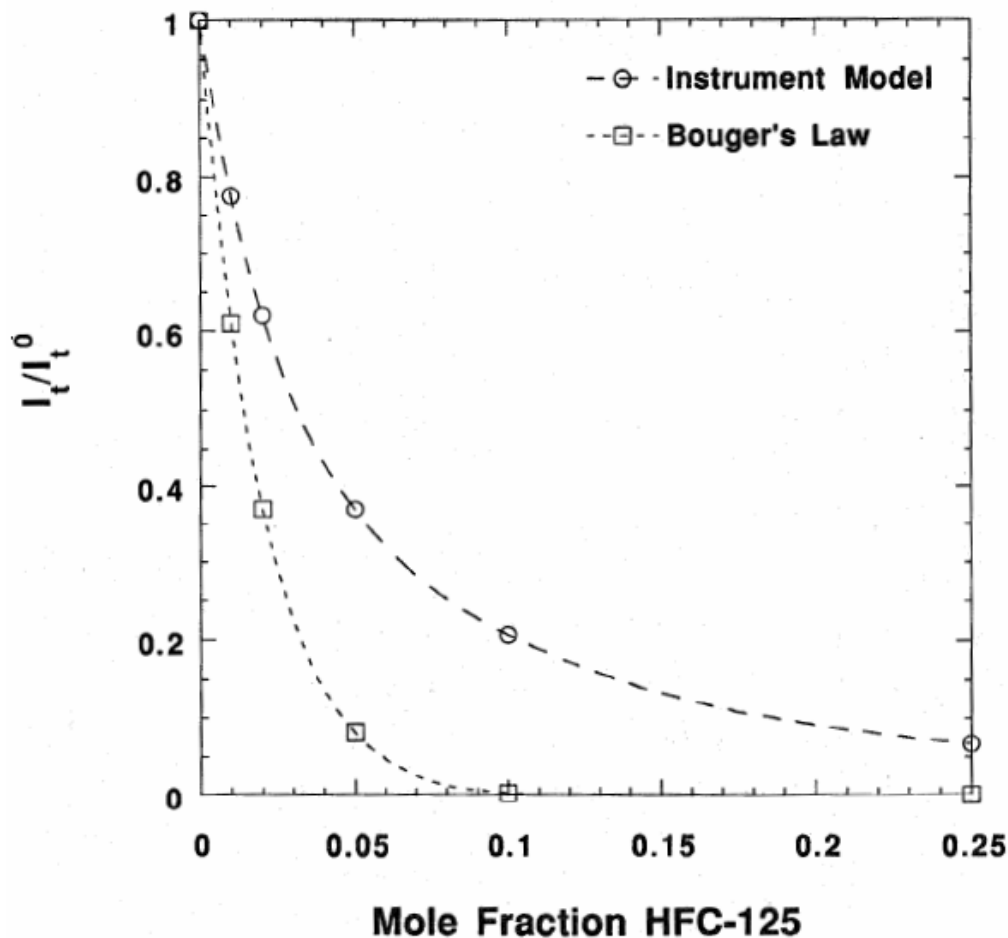
Figure 6. Comparison of the intensity ratio for the instrument (DIRRACS) and Bouger's Law versus HFC-125 volume fraction.

There are a number of secondary factors not included in the analysis that affect the instrument's performance. As the source was heated to about 800 K, the temperature of the housing was found to increase to a temperature of about 350 K over a 30 min period, and even the temperature of the conical collection tube increased from 298 K to about 303 K. The significance of this heating effect on the performance of the instrument will be discussed in the calibration section. Other factors important for quantitative modeling of the system include a spatial distribution of the source radiance, the transmission characteristics of the ZnSe and ZnS windows, and the transmission characteristics of the IR transmission tube and conical collector.

2.4   OPERATION BEHAVIOR

While calibration measurements (described in section 4.1) up to 0.25 volume fraction indicated a nominal 10 % relative uncertainty (coverage factor k=2), actual tests with a transient agent release facility indicated a systematic difference between the measured and expected values and a much larger signal noise as compared to the calibration measurements. Subsequent study indicated that the high flow velocity in the facility caused a change in the instrument response by affecting the source temperature and inducing vibrations in the instrument. An additional limitation of the method was the high background signal from the IR radiation from the walls.

Two approaches were used to correct the problems. The first approach was to surround the IR source with a cooling coil to minimize the effect of the flow on the source temperature. The second method was to use a second narrow-band pass filter at a nearby, non-absorbing wavelength. The two filters were mounted on an optical chopper so the optical signal was a composite of periods of on-feature transmittance with absorption, off-feature transmittance without absorption, and zero transmittance due to blockage of the light. In this case, it was expected that the intensities from both on- and off-feature transmittance would be affected in the same way by a change in the source temperature so that the ratio would be constant. There was some low level of absorption even at the off-feature wavelength range so the improvement was not realized. Neither method solved the flow effect problem although the cooling coil approach provided some improvement. Also, neither method corrected the problems with vibration or background radiation from the walls.

However, even with these limitations, useful data have been obtained using the DIRRACS I. Two models of the DIRRACS I were used in the first measurements of the dispersal time of an agent in the dry-bay facility at Wright-Patterson.[1] The preliminary measurements indicate that for that test, it took a relatively long time, on the order of a few seconds, for dispersal of the agent throughout the dry bay. This information has important implications about the mechanism of extinguishment when the fire is far from the release point of the agent. If the fire is extinguished under these conditions, the mechanism must <u>not</u> involve a direct interaction of the agent with the fire if one assumes the presence of the fire does not affect the distribution of the agent. These results show the value of a fast-response agent measurement. The next section describes major design changes leading to DIRRACS II.

3.0   IMPROVED INSTRUMENT DESIGN, DIRRACS II

3.1   BREADBOARDED DIRRACS II

The drawbacks of the DIRRACS I necessitated major modifications to the original design. The goals were to:
- eliminate the temperature and flow sensitivity of the source and other components,
- increase the signal-to-noise ratio, and
- increase the frequency response.

Figure 7 is a schematic of the DIRRACS II design, and Fig. 8 is a photograph of the breadboarded instrument as set up to measure a transient agent release. IR radiation is emitted by the source toward an elliptical mirror, reflected through the chopper and pinhole, collimated

by a parabolic mirror, through the periscope, reflected by a 90° mirror and a focussing mirror, through a narrow-band pass filter, and finally detected by a HgCdTe detector. The key new design features of the DIRRACS II are described below.
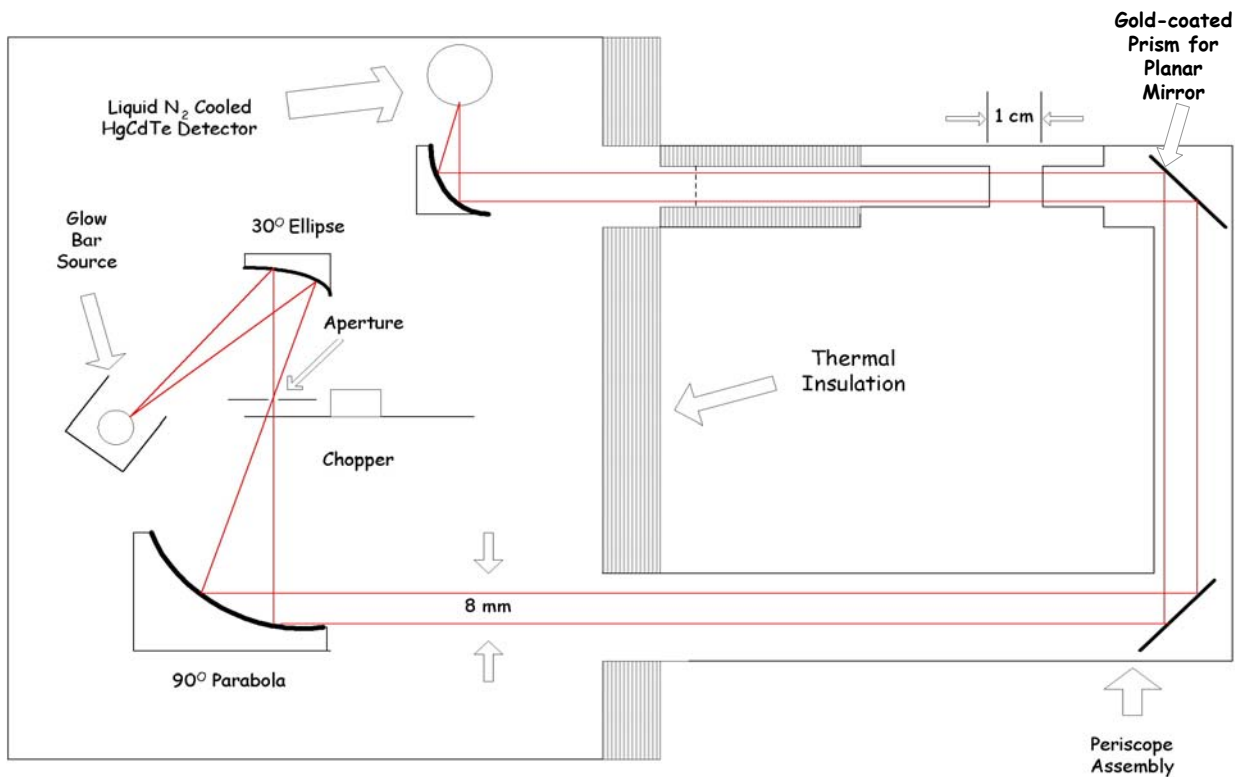
Figure 7. Schematic of DIRRACS II

To address the sensitivity of the source and other components to temperature and flow, a major optical design change was to isolate the IR light source from the flow/agent. The IR source was placed within the instrument housing to minimize the problems of high flow impacting the temperature of the source and causing source movement.

To decrease flow sensitivity as well as increase the signal-to-noise ratio, a periscope was added. The periscope was a critical design element for reducing the high noise level of the DIRRACS I induced by velocity conditions of 10 m/s to 20 m/s. A drawing of the design is provided in Fig. 9. The vibrations were greatly reduced by constructing the periscope assembly from standard stainless steel vacuum components. This structure is much more rigid than the previous optical housing. The decrease in sample path length by about a factor of two increased the practical maximum volume fraction measured by the instrument from about 0.2 to about 0.5. The periscope allows the sampling volume to be completely isolated from the rest of the instrument so convective flow and temperature variations at the measurement location cannot affect the source or detector.

Another major optical design change to increase the signal-to-noise ratio was to use a collimated IR beam instead of an uncollimated beam. Elliptical and parabolic mirrors were used to produce an 8 mm collimated beam, which passed through the periscope and was ultimately focused on

the detector. This decreased the effects of lower temperature components contributing to the radiation collected by the detector. Apparently, the background black body radiation from the walls had contributed as much as 50 % of the total IR radiation detected using the DIRRACS I design.
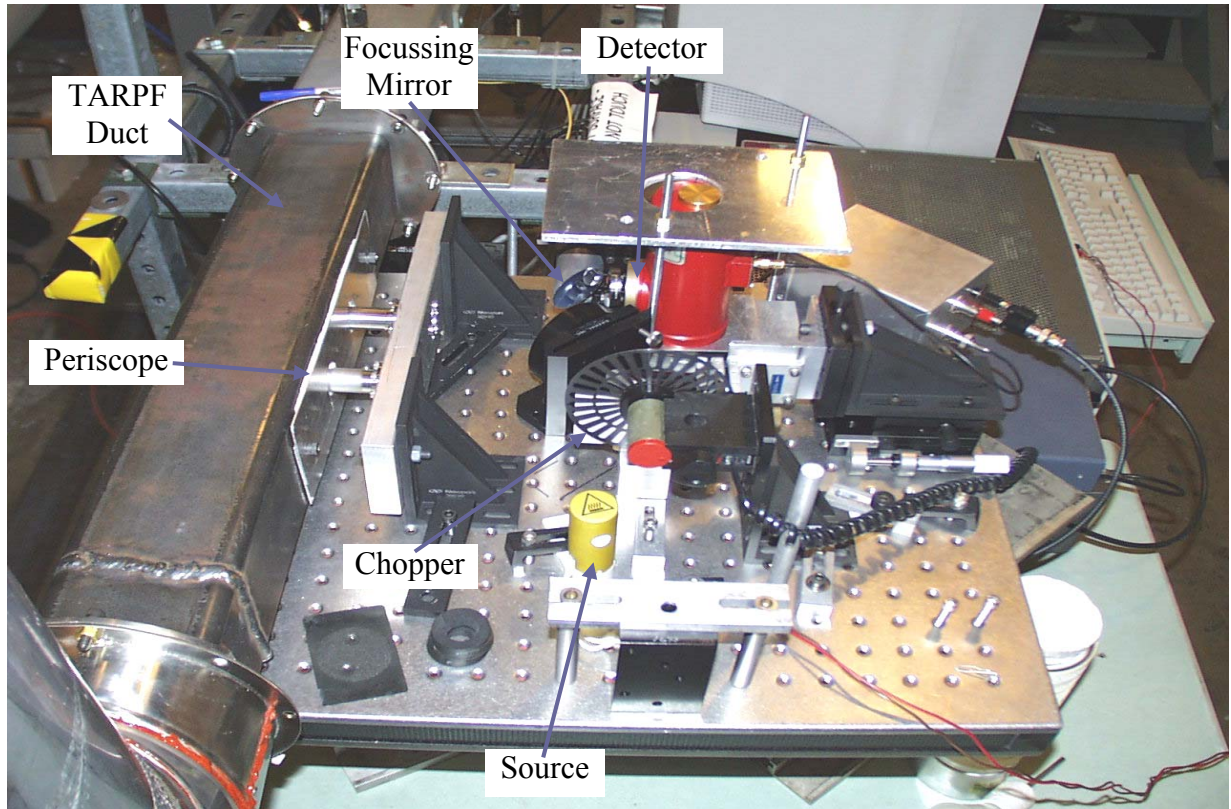
Figure 8. Photograph of the DIRRACS II with the periscope assembly mounted within the flow channel of the TARPF (Transient Application Recirculating Pool Fire) facility.

Also to enhance the signal, a better quality, high temperature IR glow bar source from a commercial FTIR (Fourier Transform Infrared Spectrometer) was used and provided a more stable output with a higher intensity at the wavelength range of interest.

High frequency operation was an important characteristic to improve in the new design in order to achieve sufficient temporal resolution to capture the details of a release event. The DIRRACS II focuses the beam through an aperture just before the chopper and uses a new, faster IR detector to allow operation of the chopper at frequencies as high as 4 kHz. The previous design with a large, unfocused beam and slow detector was limited to about 400 Hz. The responsivity (V/W) of the new HgCdTe detector improves slightly with frequency up to 5 kHz, while the previously used pyroelectric detector response falls off for frequencies above about 50 Hz. The ten-fold increase in frequency corresponds to about a ten-fold improvement in time response. The HgCdTe detector also produces a distinct, nearly square-wave output well above any background signal from extraneous radiation sources. The detector does require liquid N_2 cooling, but one filling provides at least 2 h of stable operation.
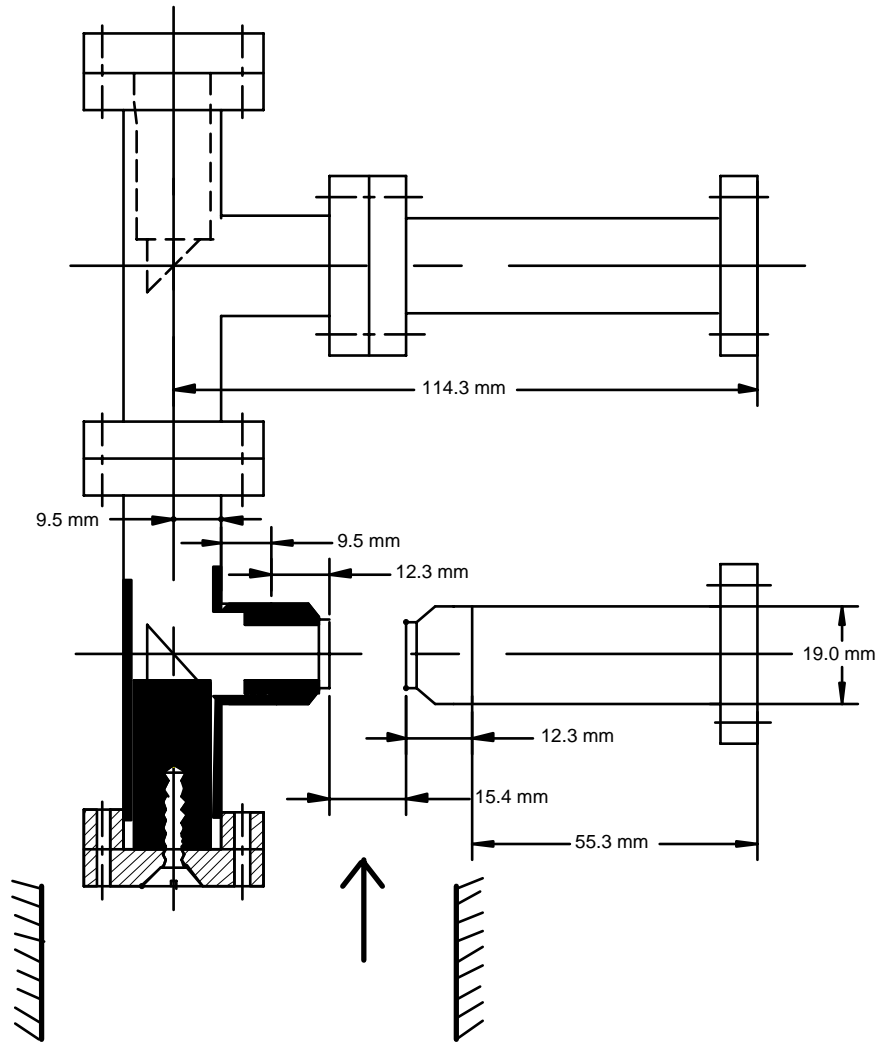
Figure 9. Drawing of the periscope.

3.2   SOFTWARE FOR DATA ACQUISITION AND ANALYSIS

In addition to the hardware design improvements, improvements to data acquisition and analysis were also made. The old DAQ board was limited to about 20 kHz sampling frequency. The new DAQ board allows variable data collection rates up to 250 000 samples/s. Typically, a setting of 128 000 samples/s was used to allow data to be collected over a longer time period for a given level of data storage. Either an internal or external trigger can initiate data collection. The previous method of analysis involved post-processing of the data which required at least an hour. The current software combines the functions of acquisition and analysis. In conjunction with a faster computer and new data acquisition board, the software reduces the data and displays it within 20 s after acquisition. The software performs preliminary filtering using Fast Fourier Transform (FFT) analysis to remove DC offset, drift, and 60 Hz noise. The software performs the filtering using digital lock-in amplification with the frequency determined by the chopper reference output and averages over a discrete and selectable number of cycles.

The analyzed data can be displayed in two formats. The first display consists of a plot of the raw voltage signal versus time and a plot below it of the chopper output versus time. The user can toggle back and forth between the two plots displayed. An example of this display is shown in Fig. 10. Figure 11 shows the peak-to-valley voltage data after processing for an agent release event. The signal deflection due to absorption is apparent in the upper plot.

Figure 10. The screen display for the data acquisition and processing software. It shows a plot of the raw signal generated by the DIRRACS II. It is zoomed to a time range of 10 ms. The lower plot is the reference signal generated by the chopper.

The software also allows zooming in on specific time periods and changing scales on the plots. The software allows both the raw data and the analyzed data to be exported for use with various standard software packages for additional plotting and statistical analysis. Currently, the calibration curve relating the peak-to-valley voltage and the agent concentration is not automatically applied using the DAQ/analysis software.

3.3   DIGITAL SIGNAL PROCESSING

The purpose of the digital data processing described below is to obtain the amplitude of the measured signal as a function of time. The whole procedure can be imagined as a kind of software implemented "lock-in" filtration, where the square-wave signal from the chopper is used as a reference and the waveform from the detector is considered as a signal input.

12
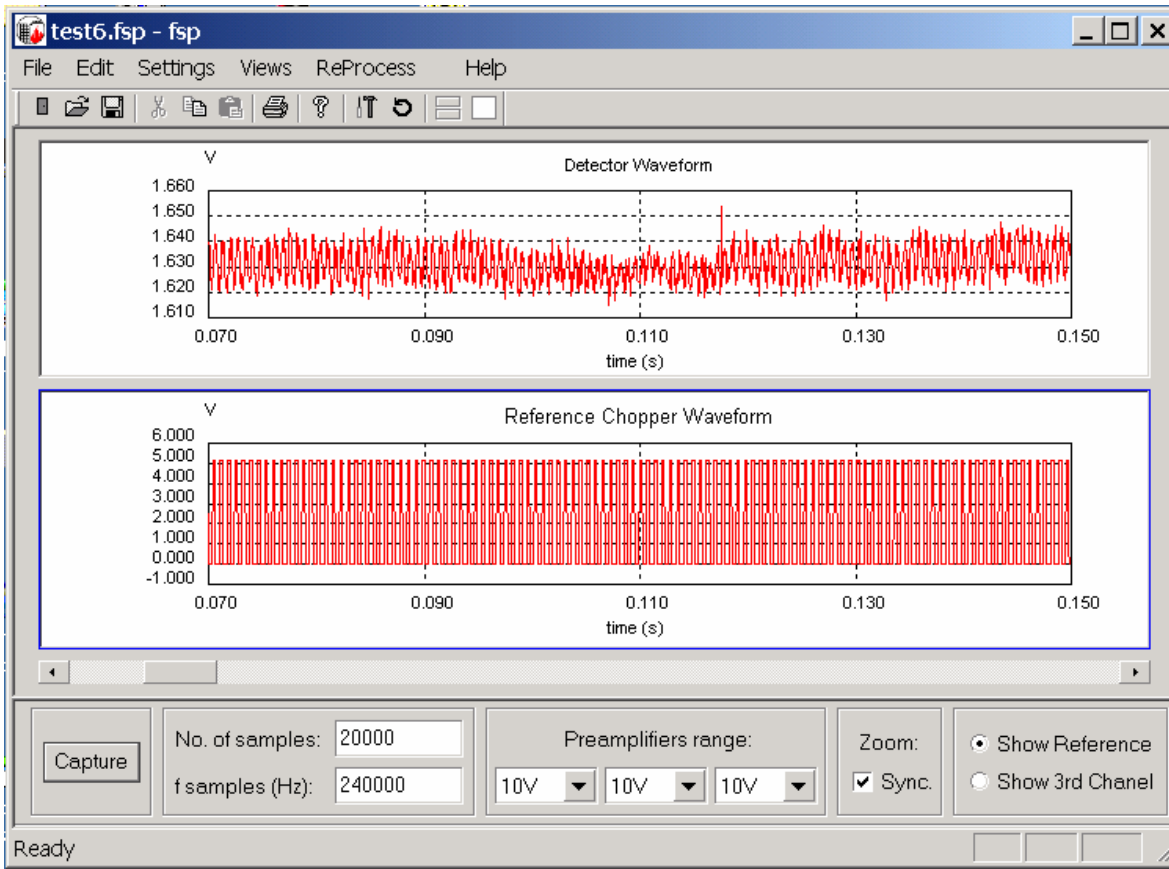
Figure 11. Data after processing which shows signal deflection during absorption event.

The digital part of the system consists of a 400 MHz Intel Pentium II based PC working under the Windows 98 operating system, a National Instruments multifunction board (PCI-MIO-16E-1 with PCI interface), and original software written for the experiment. The board works as a three-channel analog-to-digital converter. One channel is for the signal from the infrared detector, the other one is for the reference signal from the optical chopper, and the third channel is designed for monitoring any other voltage output depending on the experimental requirements. Data acquisition can be started either by the software (soft trigger) or by an external TTL signal (external trigger). The maximum rate of the simultaneous three channel sampling that can be set by the software is 200 000 samples per second.

The system software is a Windows native Win32 GUI application developed using Microsoft VC++ and MFC. The application controls the PCI-MIO-16E-1 data acquisition board using the National Instruments NI-DAQ driver software.

The processing procedure consists of two stages: preliminary filtering and lock-in filtering. The purposes of preliminary filtering are: (1) to separate significant information in the measured signal from interference such as DC offset and drift, power line 60 Hz frequency, etc.; and (2) to convert the processed data into the form of an analytical (complex) signal by calculating the Hilbert Transform [7]. The following derivation provides an overview of the digital lock-in and filtering algorithm we used.

13

The filtering algorithm is a FFT based complex filtration in the frequency domain. The IFFT (Inverse Fast Fourier Transform) procedure is calculated to convert processed data back to time domain. Let $X\{n\}$ be the chopper output data set which represents the reference waveform for the lock-in procedure, where n is an integer ranging from $0....N\text{-}1$. The program routine chooses some subset of $X\{n\}$ so that the length of this new data set would be a number $L = 2^m$, where L is the first integer greater than N taken from the 2^m set, and m is an integer. The end part of the new data set $\widetilde{X}$ from $\widetilde{X}_N$ to $\widetilde{X}_{L-1}$ is filled by "0" (zeroes). Then, $\widetilde{X}\{n\}$ is treated by the FFT algorithm to map the data set from time sequence into the frequency domain, and after that the amplitude spectrum of $\widetilde{X}$ is calculated also:

$$S\{k\} = FFT(\widetilde{X}\{n\}) \qquad n = 0...L-1; \quad k = 0...L-1 \qquad (8)$$

$$\hat{S}\{k\} = |S\{k\}| \qquad k = 0...L-1 \qquad (9)$$

Where:

$\widetilde{X}\{n\}$ - is the L length subset of $X\{n\}$,

$S\{k\}$ - is the FFT of $\widetilde{X}\{n\}$,

$\hat{S}\{k\}$ - is the amplitude spectrum of $\widetilde{X}\{n\}$,

and L - is the FFT length.

Then the routine searches for the index i_m, corresponding to the maximum value of $\hat{S}\{k\}$ in the index range i_s - i_e, where: i_s is the integer low cut-off frequency index, and i_e is the integer high cut-off frequency index, which is equal to $L/2$. This index i_m is used to center the complex band pass filter which can be implemented as a weight function in frequency domain:

$$H\{i\} = \frac{1}{1 + ((i - i_m)/hw)^2} \qquad (10)$$

Where:

$H\{i\}$ - is the filter band pass weight function,

hw - is the filter band pass half width,

i - is the frequency domain data set index,

and i_m - is the index i of the maximum of $\hat{S}\{k\}$.

The final stage of this filtration is multiplying the spectrum of the source data by a filter weight function and than calculating the IFFT to map the treated data back to time domain, as shown below:

$$Y\{k\} = IFFT(S\{n\} \cdot H\{n\}) \qquad n = 0...L-1; \quad k = 0...L-1 \qquad (11)$$

Where:

$H\{n\}$ - is the filter band pass weight function,

14

$S\{n\}$ - is the FFT spectrum of $\widetilde{X}\{n\}$,

and $Y\{k\}$ - is the reference data set after treatment.

The treated data set $Y\{k\}$ has real and imaginary components and an envelope function independent from the beginning phase, which may be uncertain in the source data set.

The lock-in filtering is a standard procedure where a low pass filter treats detector channel data multiplied by reference data. Output of this low-band pass filter reflects the amplitude of the original signal.

$$Dm\{k\} = \frac{1}{Lf \cdot Py} \cdot \left| \sum_{n=k}^{k+Lf} (D_n \cdot Y_n) \right| \qquad k = 0...N - Lf - 1 \qquad (12)$$

Where:

$D\{n\}$ - is sampled data from detector output,

$Y\{n\}$ - is the preliminary filtered reference waveform,

Lf - is the length of sliding summation,

Py - is the normalization coefficient,

and $Dm\{k\}$ - is the final data set after processing.

The coefficient Py can be calculated as:

$$Py = \frac{1}{Lf} \cdot \sum_{n=k}^{k+Lf} |Y_n| \qquad (13)$$

The value of Lf is software selectable. It has to be an integral number of sampled cycles of the periodic chopper reference waveform. This is provided by the following calculation:

$$Lf = \text{int}(La / lc) \cdot lc \qquad (14)$$

Where:

Lf - is the actual length of sliding summation,

La - is the approximate value of Lf, selected from the series 64, 128, 256, 512,

and lc - is the number of points per chopper waveform cycle.

The value of lc is calculated as:

$$lc = \text{int}(L \cdot i_m) \qquad (15)$$

Where:

L - is the FFT length defined in (8), and

15

i_m - is the index of the maximum of the amplitude spectrum $\hat{S}\{k\}$ of the chopper waveform determined at the preliminary filtering stage. See Eq. (10).

3.4   COMPACT/HARDENED DIRRACS II

3.4.1   Hardware Changes

The next stage of development of the DIRRACS II was the assembly of a portable version to be deployed for field experiments. The plan was to shrink the spaces between the optical components and, as possible, obtain more compact versions of the components. A housing was constructed to provide better electronic isolation as well as to protect the instrument from dust and debris generated in release tests. The footprint (excluding the periscope) of the new version decreased from 48 cm x 58 cm to 22 cm wide x 31 cm long x 18 cm high through a careful repositioning of the same or smaller components.

Figure 12 is a view from the top of the internal components of the instrument. The location of the IR source, a focusing mirror, a second mirror for creating a uniform beam, and the liquid nitrogen Dewar are shown in the figure. The HgCdTe sensing element is attached on the far side of the Dewar and is not visible. Also apparent is the chopper blade positioned just after an aperture. The periscope assembly is seen extending outside the instrument chassis in the upper right hand corner. A portion of the 1 cm sample path length is visible just to the right of the lower section of the periscope assembly. The ruler near the periscope has major gradations of 1.27 cm (0.5 in).

The chopper controller and the power supplies are located outside the box up to 1 m away. The data acquisition software was modified to gather data from 3 channels: the transmitted IR beam intensity, chopper frequency, and also agent cylinder pressure.

Two precautions were taken to prevent the possibility of agent leakage through the periscope windows or into the housing and main optical path. First the window seals were checked and found to be airtight. Second, N_2 was continuously metered into the DIRRACS II housing to maintain a positive, internal pressure to prevent leakage of agent into the housing or periscope and minimize background atmosphere absorption. This was accomplished by plumbing the housing with an inlet, outlet, pressure gauge, and rotameter. The flow of N_2 was set to about 0.1 L/min.

3.4.2   Performance Issues

The DIRRACS II had experienced some variation of the calibration from day to day (about ± 2 % voltage output for a given concentration). Attempts were made to diagnose the source of the variation with the anticipation that a design solution could be applied to the hardened DIRRACS II. The calibration facility was checked carefully. Also, the flow-through calibration cell was redesigned to minimize volume and the time response to a step change in concentration. The variation was eventually attributed to drift in the preamplifier circuitry. Two fixes were proposed, but neither has been implemented as of this writing. The first was a hardware change: installing a higher precision amplifier with lower drift characteristics and DC coupling. This

would also allow elimination of intermediate capacitors which are not recommended for the particular ADC (analog-to-digital converter) board with input multiplexer being used. A second proposed fix to improve stability was to increase the accuracy (and complexity) of the software processing algorithm which requires a faster processor to maintain the existing response time.
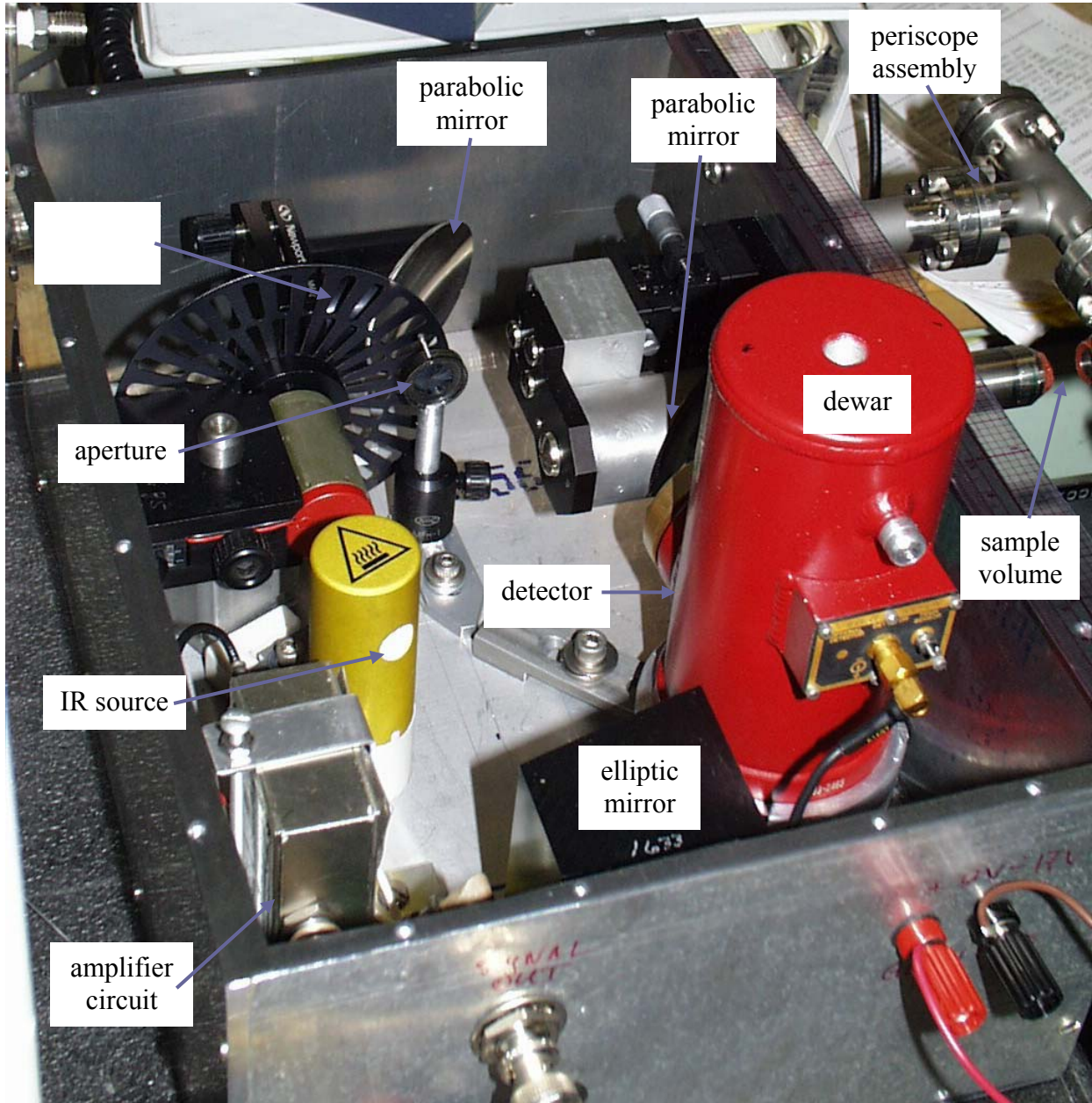
Figure 12. Photograph of the interior of the hardened, compact DIRRACS.

In summary, extensive changes were made to the breadboarded DIRRACS II to make the compact/hardened version. The primary changes consisted of shrinking the spaces between components and placement of the main optics in a sealed, pressurized, sturdy housing with access to the sampling volume through the periscope. Variations in calibration behavior were investigated, and solutions for eliminating the inconsistency were recommended.

17

4.0   EXPERIMENTS AND RESULTS

4.1   CALIBRATION

Calibrations of the DIRRACS II were conducted with a facility described in detail by Pitts *et al.* [1]. Only a summary of the apparatus and procedure are presented here. The calibration facility consists of 3 mass flow controllers and various solenoid and pneumatic valves controlled with a computer, data acquisition board, and analog/digital output board. One 2 L/min (maximum) and one 10 L/min mass flow controller are used to meter the agent through the system. The programming prescribes at what point the fraction of agent in the mixture is best supplied through the higher capacity controller. The third controller is a 10 L/min model which is dedicated to air flow.

The program uses equations based on calibrations of each flow controller for agent or air to set the mass flows to match the selected mass fraction of agent. The system output changes the mixture at the calibration cell within seconds. The sealed cell with an inlet and outlet for agent/air mixture flow was attached to the DIRRACS II periscope around the sampling volume. Because leakage of agent into the periscope through the window seals was suspected with the breadboarded DIRRACS II, 120 kPa pressure air was blown (indirectly, not sealed) into the two periscope ends to prevent accumulation of agent which would impact the calibration. With the hardened DIRRACS II, the N_2 purge accomplished the same goal. Since the cell was not designed for the DIRRACS II, it had a relatively large interior volume and required about 1 min for a mixture to completely change to a new mixture input by the operator.

Preliminary calibration of the breadboarded DIRRACS II was conducted to prove that it was functioning properly before continuing with the next stage of development of the compact/hardened version. The new version was calibrated more rigorously as an actual prototype for field use. Data from three separate calibrations of the DIRRACS II for HFC-125 are shown in Fig. 13. The normalized average peak-to-valley voltages are plotted versus agent volume fraction, and the curve fit for all of the data is shown. Each data point represents an average of data collected over 1 s. The standard deviations for 1 s samples of data generated with particular calibration mixtures ranged between 0.1 % and 0.25 % of the averages.

The expanded combined relative standard uncertainty (2 standard deviations) among the average peak-to-valley data points shown in Fig. 13 is about 2 % of nominal for the calibrations that were conducted, which translates into a 0.005 volume fraction uncertainty. It was later determined after development and testing of the compact model that preamplifier drift was responsible for variations from one calibration to the next.
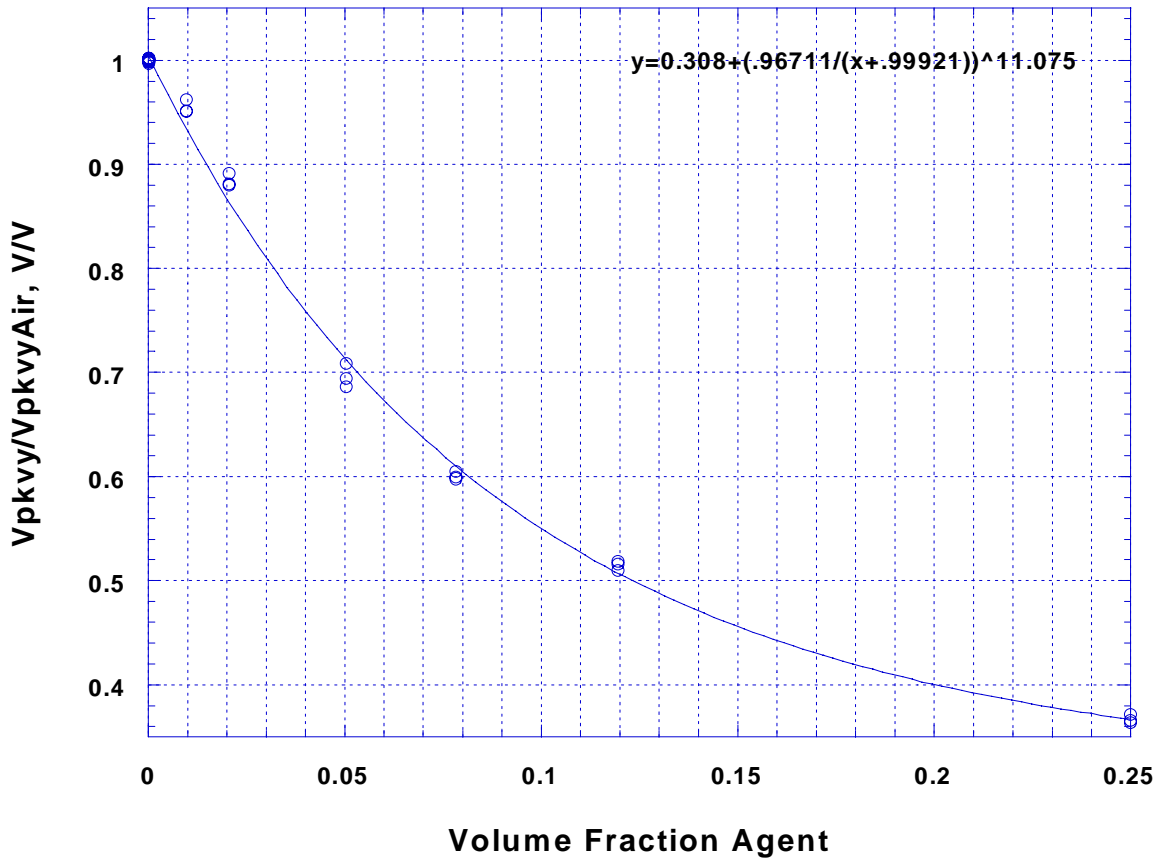
Figure 13. A compact DIRRACS II calibration plot of average normalized peak-to-valley signals versus the volume fraction of HFC-125. Error bars for the averages are smaller than the symbols.

4.2 AGENT RELEASE TESTS AT NIST

4.2.1 Experiments

Releases of HFC-125 were conducted in the Transient Application Recirculating Pool Fire (TARPF) facility at NIST. The facility is more completely described in Grosshandler *et al.* **[8,9]**. A schematic diagram is shown in Fig. 14. The facility consists of a 2.5 m long duct of 9.2 cm x 9.2 cm square cross section which is connected to a high capacity air compressor. Variable orifice plates allow the compressor to generate air velocities up to 20 m/s in the duct. Various agents can be stored in 1 L and 2 L cylinders. Before a test, a cylinder is filled to a prescribed pressure, which is measured with a pressure transducer inside the cylinder. A release is controlled with a timer that determines the length of time the cylinder solenoid valve is opened. The normal operation of the TARPF facility consists of igniting a flame in a test section and releasing various amounts of agent upstream to observe the extinguishment behavior. For the DIRRACS II (breadboarded) testing, no flame was ignited, but the air flow and agent release capabilities of the system were used. The periscope assembly was mounted 0.5 m downstream of the pool fire zone and about 2 m downstream of the region where the agent is mixed into the air stream.
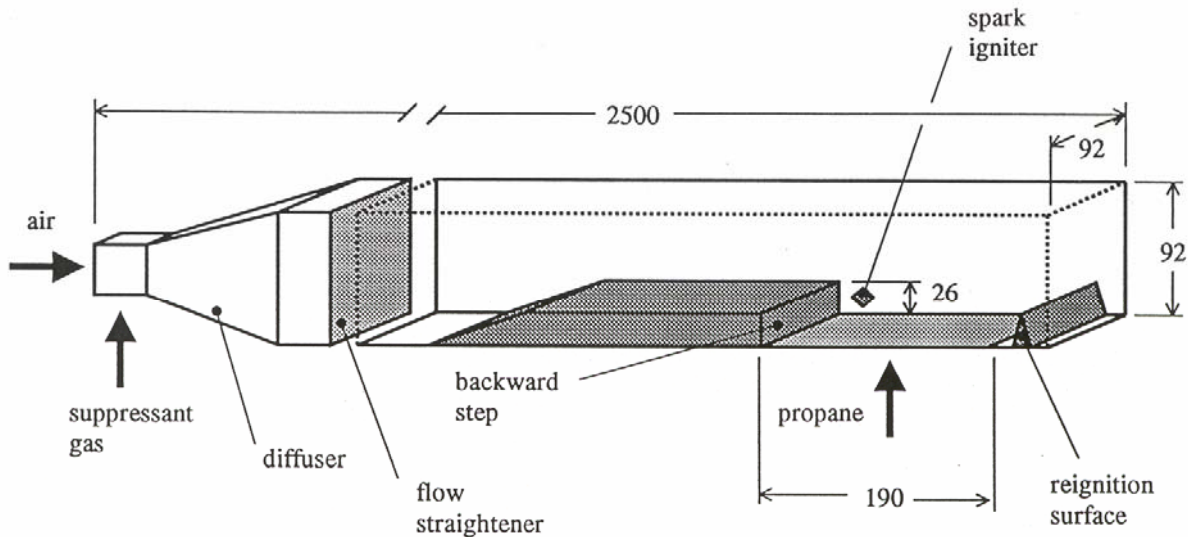
Figure 14. A schematic of the TARPF facility at NIST used to conduct release experiments monitored by the breadboarded DIRRACS II. Dimensions are in mm. **[7,8]**

Over 40 release tests were conducted in the TARPF facility. Each test was conducted with specified settings of air flow, agent vessel pressure, and agent vessel valve opening period. In order to capture events of less than 1 s with the data acquisition system, varying combinations of total points collected and sampling frequency were used. The series of tests with the DIRRACS II was used to help characterize the distortion of pulses of agent as they moved downstream after each release. Only two tests are described here as typical of those in the series.

4.2.2 Results

Figure 15 shows the results obtained from two releases of the HFC-125 agent in the TARPF facility. The first was a 100 ms pulse with a 30 kPa initial agent pressure (P_i), and the second was a 250 ms pulse with a 330 kPa pressure. The air velocity through the duct was 11 m/s. The ordinate is the peak-to-valley voltage normalized by the background value which is proportional to the IR intensity incident on the detector. The abrupt decrease in the voltage is a result of the IR absorption by the HFC-125. The width of the decrease in the voltage is significantly larger than the release time because of downstream mixing effects.

The plot of volume fraction versus time for the same experiments as Fig. 15 is shown in Fig. 16. The different pulse durations are apparent, although the step releases become significantly spread out. These two tests represent the conditions near the extremes that were tested. The test data indicate that a 0.005 volume fraction of HFC-125 can easily be detected and differentiated from background noise. Also, turbulent fluctuations on the order of 5 ms to 10 ms are clearly resolved due to a combination of the 2 kHz chopping frequency and the Fourier transform high frequency filtering. For just air flowing past the periscope in the TARPF facility, the standard deviation normalized by the average of a 1 s sample of the peak-to-valley signal data was typically about 0.2 %. This is a substantial improvement over the DIRRACS I, which had a standard deviation of 23 % under the same conditions.

20
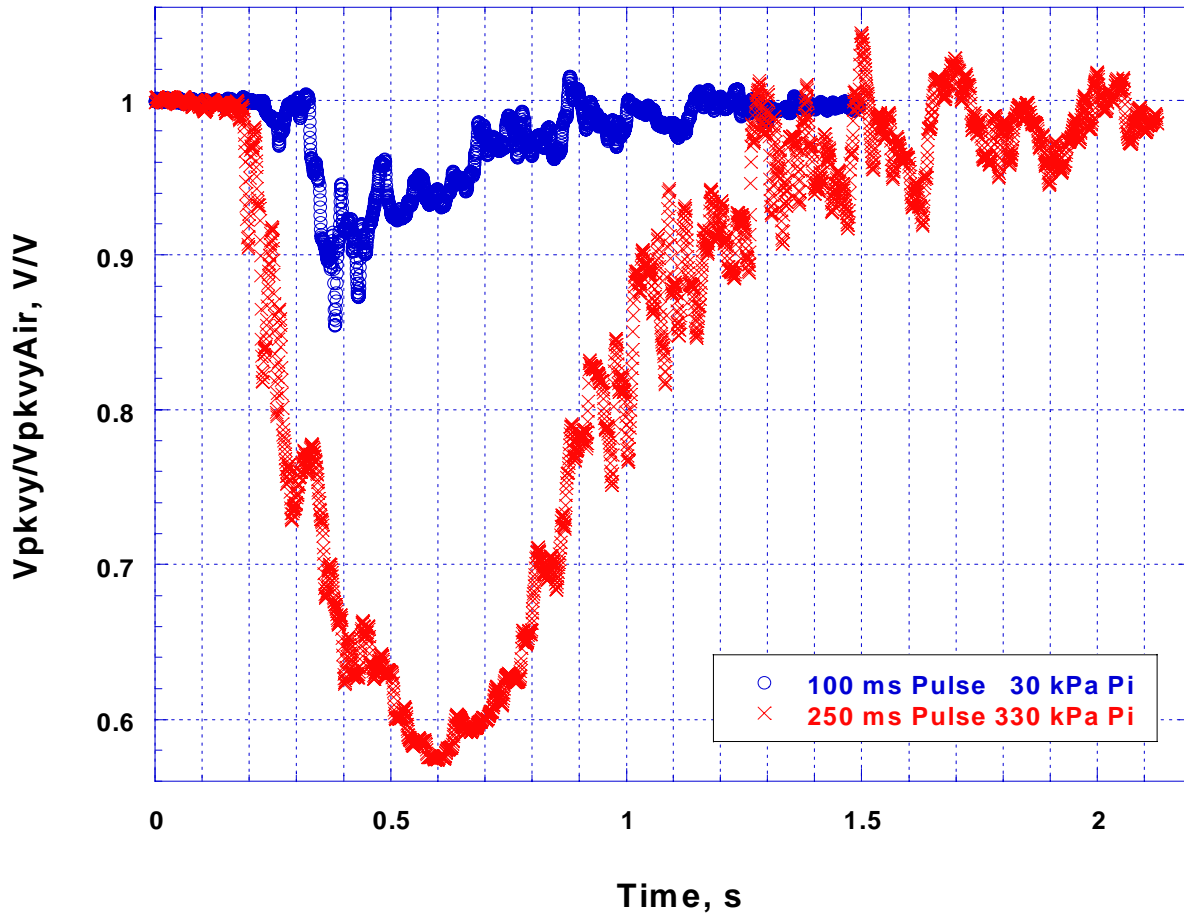
Figure 15. A plot of normalized peak-to-valley signals resulting from processing the raw signal from the compact DIRRACS II generated from two HFC125 releases with chopping frequency of 2 kHz and sampling frequency of 128 kHz.

4.3   AGENT RELEASE TESTS AT ABERDEEN

The performance of this instrument has been assessed based on tests conducted at Aberdeen Proving Ground, MD through the Aberdeen Test Center, ATC. The following sections describe the tests and results, especially with regard to the instrument's response to temperature and flow effects during transient agent concentration measurements.

4.3.1   Experiments

Before the compact DIRRACS II was taken to the ATC for testing, a series of calibrations was performed. The equation relating the output signal to agent concentration changed numerically from the breadboarded version, but was qualitatively the same. The difference in the calibration curve was expected due to the changes in the optics and especially due to variations in focusing the beam on the detector.
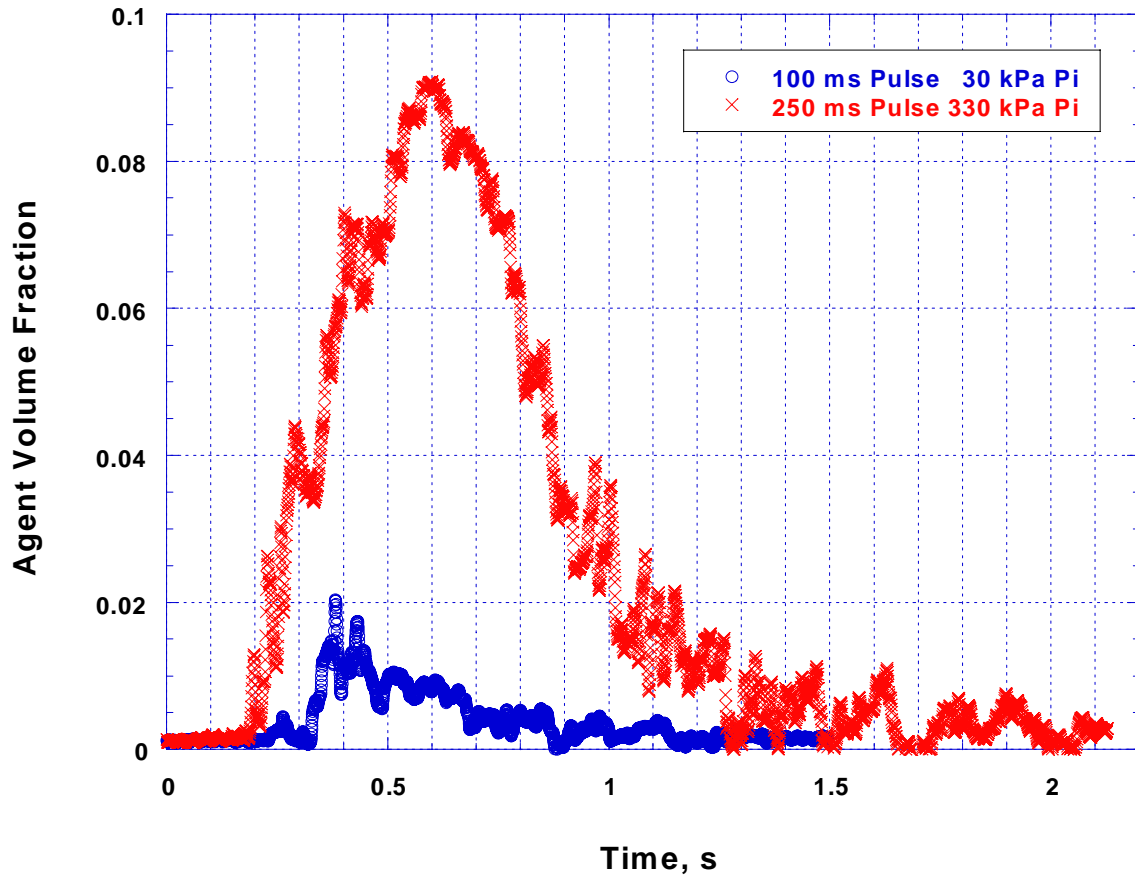
Figure 16. A plot of HFC 125 agent volume fraction versus time for two releases of
HFC-125 in the TARPF facility.

A series of 11 tests were carried out in a Bradley armored personnel carrier modified for testing
agent release and fire suppression. The vehicle is shown in Fig. 17. The extinguishing agent,
HFC-125, was released in amounts ranging from about 2 kg up to about 4 kg at a fill pressure of
5.2 MPa. All of the releases were from the right, high mounting position just behind the turret.
The concentration was monitored at a high location, which was near head height for an occupant
of the vehicle, and a low location, which would be about waist height. Figure 18 shows the
DIRRACS II positioned at head height in the left rear of the compartment about halfway back
from the turret to the rear of the tank. The instrument is located between two rectangular
structures representing the location and approximate size of two occupants of the vehicle.

4.3.2   Results

The agent volume fraction and the cylinder pressure are plotted versus time for the DIRRACS II
in the high position in Fig. 19. The HFC-125 reaches the measuring position about 300 ms after
the release. The peak agent volume fraction is 0.22 and decreases to a value of about 0.07 after
1.5 s. Figure 20 provides a comparison for the results for the DIRRACS II in the upper and
lower location. In the lower position, the arrival time increases from 300 ms to about 400 ms,
the peak volume fraction decreases to about 0.12; however, after 1.5 s the volume fraction is
slightly higher at the lower position, 0.09 compared to about 0.07. After 2 min the HFC-125

volume fraction was in the range 0.03 to 0.09 compared to an estimate of 0.095 based on a well mixed distribution throughout the volume of the vehicle.

Figure 17. Bradley armored personnel carrier modified for performing agent release and fire suppression studies.

Figure 21 shows the same release as Fig. 19. The time axis is focused on the first 300 ms of the test and the upper position agent volume fraction and cylinder pressure are displayed. The plot shows that the background volume fraction experiences larger fluctuations after 115 ms due to the pressure pulse effect on the instrument. The actual agent arrival occurs at about 275 ms. The background volume fraction is close to zero and averages about 0.0006. The magnitude of the background fluctuations with the pressure effect is about 3 times that of the background fluctuations before the effect. After arrival of the agent, the volume fractions range between 0.05 and 0.21 (see Fig. 19) which overwhelms by two orders of magnitude the background level and by at least a factor of 25 the effect of pressure or vibration noise.

5.0   CONCLUSIONS/IMPORTANT FINDINGS

DIRRACS II meets the design needs for monitoring halon replacement chemicals. One goal was to develop an instrument for measuring agent concentration during a release with a 10 ms time response, which is thought to be fast enough to allow the quantification of the transient agent concentration during the suppression of the fastest fires involving military systems. It has been demonstrated that the DIRRACS II meets and exceeds this objective by using a 2000 Hz

chopping speed together with a fast-response HgCdTe detector. The DIRRACS II can monitor the agent releases with a 4 ms time response and can capture the structure of distinct events that are less than 10 ms in duration. The DIRRACS II time response is useful for slowly or quickly changing conditions.

Figure 18. The "high" location of the DIRRACS-II and the periscope is shown to be located between two rectangular structures simulating occupants.

The other design goal was to measure agent concentration over the range from 0.01 to 0.20 with an expanded uncertainty of 10 % of the nominal value. The DIRRACS II can measure agent concentration from 0.01 to 0.25 with a 0.005 uncertainty. This meets the design goal for concentrations greater than 0.05. A more stable amplifier circuit would extend this performance over the full range. The DIRRACS II can be used for any agents with the C-F bond using the current filter or replacing it with one more closely matched to an agent's absorption spectrum.
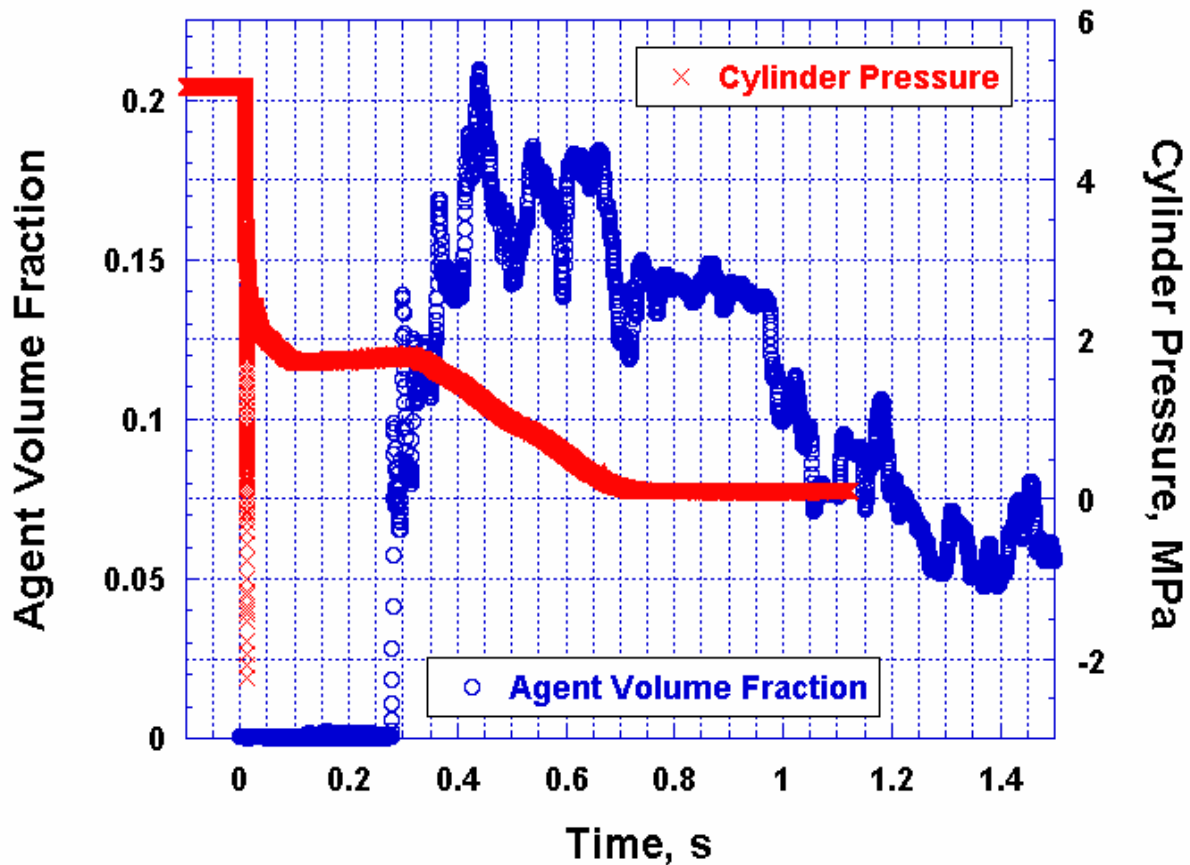
Figure 19. HFC-125 volume fraction and cylinder pressure versus time at the upper
measurement position.

It was demonstrated that a much smaller portable DIRRACS II could be fabricated and
successfully deployed to monitor the agent concentration release in a Bradley vehicle. One
significant finding was that the times for the agent to reach the measuring positions were about
300 ms and 400 ms for the upper and lower position in the vehicle, respectively. This
demonstrated the capability of the instrument to resolve the different agent arrival times at the
two locations. The transit time of the agent appears to be longer than the desired time to
extinguish the fire. This information could be useful for understanding the mechanism of fire
suppression for the fire tests performed in the Bradley vehicle.

The demonstrated capability of the DIRRACS II to monitor HFC-125 concentration with a 4 ms
time response over the volume fraction range from 1 % to 25 % leads to its potential use in full-
scale agent release testing applications. The design is ready to be adapted for reproduction or
commercialization. A manual [10] has been prepared to assist in the fabrication of copies of
DIRRACS II and to provide operation instructions to users. The DIRRACS II could be useful
for monitoring agent concentration in a flame environment provided some protection is added to
shield the periscope and other exposed components from the corrosive gases produced by agent
and fire interaction.
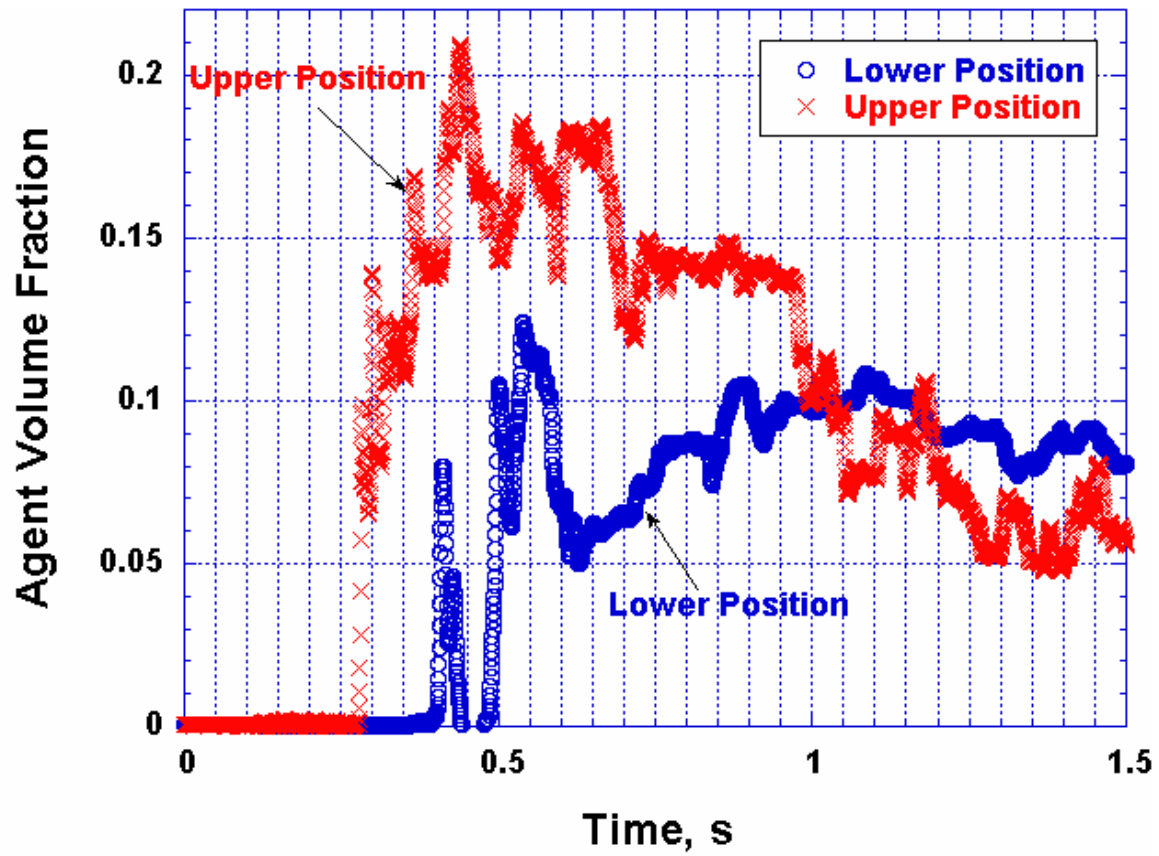
Figure 20. Two releases of 3.5 kg of HFC-125; one with the DIRRACS-II in a high position and one in a low position.
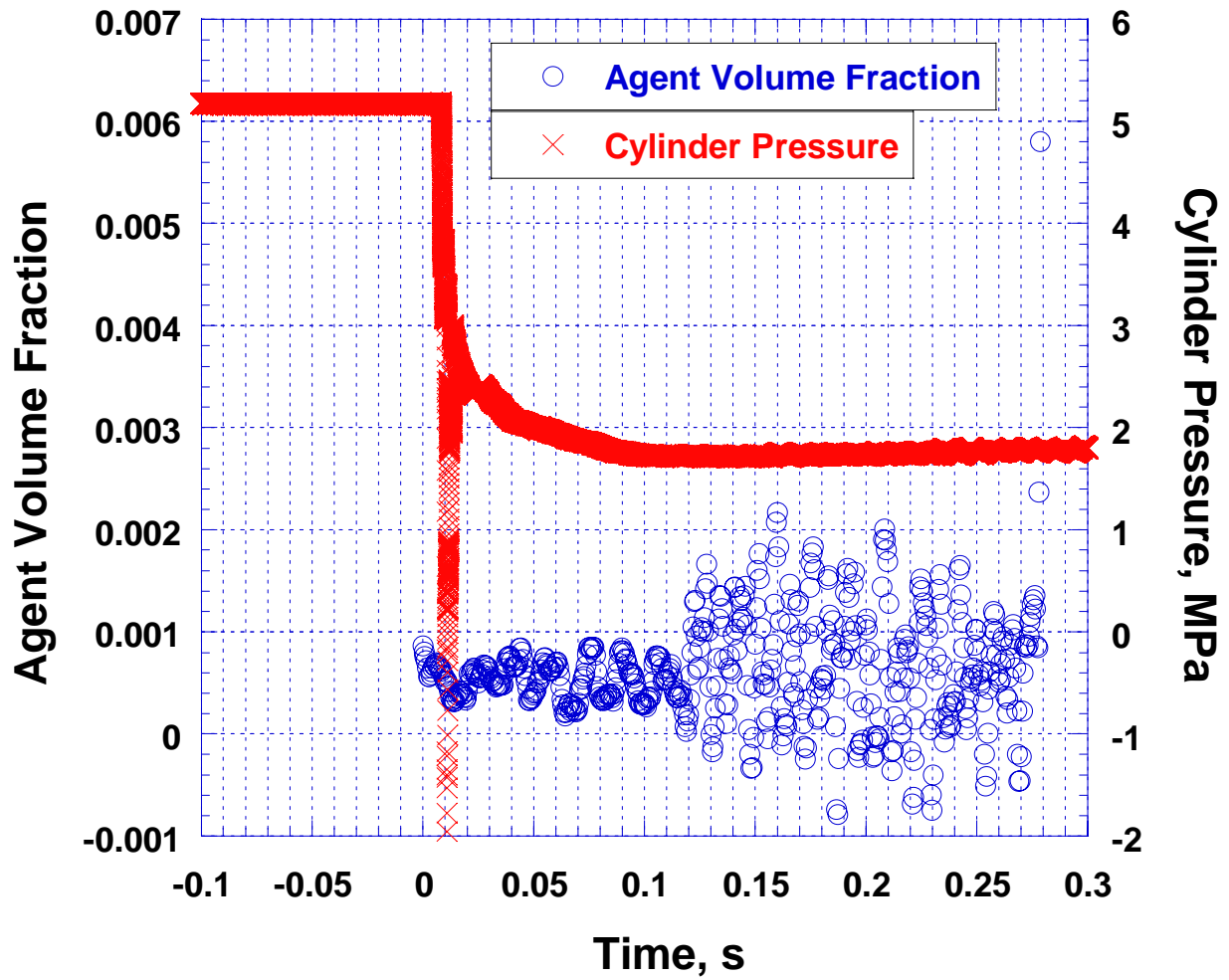
Figure 21. Agent volume fraction versus time showing the pressure pulse arrival at the DIRRACS II (115 ms) before the agent arrival (275 ms).

REFERENCES

1. Pitts, W. M.; Mulholland, G. W.; Breuel, B. D.; Johnsson, E. L.; Chung, S.; Harris, R. H., Jr.; Hess, D. E., **"**Real-Time Suppressant Concentration Measurement," in *Fire Suppression System Performance of Alternative Agents in Aircraft Engine and Dry Bay Laboratory Simulations. Volume 2 (*Gann, R. G., Editor), NIST SP 890, National Institute of Standards and Technology, Gaithersburg, MD, November 1995.

2. Pacific Scientific HTL Division, *Halonyzer II Operation/Maintenance,* Document No. 57180001, September, 1988a.

3. Yanikoski, F. F., "Gas Analysis Apparatus", United States Patent Office Patent Number 2,586,899, February 26, 1952.

4. Takeuchi, K.; Tanaka, T.; Ikeda, M.; Shibata, K.; Sakauchi, Y; Yamada, Y.; and Nakano, S., "Highly Accurate CO_2 Gas Sensor Using a Modulation Type Pyroelectric Infrared Detector," *Jpn. J. Appl. Phys. 32*, 221 (1993).

5. McGee, P. R.; Cleveland, F. F.; and Miller, S. I., "Infrared Spectral Data and Tentative Assignments for CF_3Br and CF_3I," *J. Chem. Phys. 20*, 1044 (1952).

6. Dereniak, E. L. and Crowe, D. G. Optical Radiation Detectors. Wiley, New York, 1984.

7. Bracewell, R. N. The Fourier Transform and Its Applications. McGraw-Hill Book Company, Singapore, International edition, 1986, pp 267-74.

8. Grosshandler, W. L.; Donnelly, M. K.; Charagundla, S. R.; Presser, C., "Suppressant Performance Evaluation in a Baffle-Stabilized Pool Fire," in *Halon Options Technical Working Conference. Proceedings. HOTWC-99*, Albuquerque, NM, April 27-29, 1999.

9. Grosshandler, W., Hamins, A., Yang, J., McGrattan, K., and Presser, C., "Transient Application, Recirculating Pool Fire, Agent Effectiveness Screen: Final Report," in *Halon Options Technical Working Conference. Proceedings. HOTWC-01*, April 24-26, 2001, Albuquerque, NM, (2001).

10. Johnsson, E. L.; Mulholland, G. W.; Fraser, G. T.; Leonov, I. I.; and Golubiatnikov, G. Y., "Description and Usage of a Fast-Response Agent Concentration Meter," NIST TN XXXX, National Institute of Standards and Technology, Gaithersburg, MD, August 2004.